Talanta 84 (2011) 783–788

Contents lists available at ScienceDirect

Talanta

journal homepage: www.elsevier.com/locate/talanta

Fe_3O_4 nanoparticles-enhanced SPR sensing for ultrasensitive sandwich bio-assay

Jianlong Wang, Zanzan Zhu, Ahsan Munir, H. Susan Zhou*

Department of Chemical Engineering, Worcester Polytechnic Institute, 100 Institute Road, Worcester, MA 01609, USA

ARTICLE INFO

Article history:
Received 13 January 2011
Received in revised form 7 February 2011
Accepted 9 February 2011
Available online 19 February 2011

Keywords:
Magnetic nanoparticles
Surface plasmon resonance
Sandwich bio-assay

ABSTRACT

Magnetic nanoparticles (MNPs) have been receiving increasing attention because of its great potentials in bioseparation. However, the separation products are difficult to be detected by general method due to their extremely small size. Here, we demonstrate that MNPs can greatly enhance the signal of surface plasmon resonance spectroscopy (SPR). Features of MNPs–aptamer conjugates as a powerful amplification reagent for ultrasensitive immunoassay are reported in this work for the first time. In order to evaluate the sensing ability of MNPs–aptamer conjugates as an amplification reagent, a sandwich SPR sensor is constructed by using thrombin as model analyte. Thrombin, captured by immobilized antithrombin aptamer on SPR gold film, is sensitively detected by SPR spectroscopy with a lowest detection limit of 0.017 nM after MNPs–aptamer conjugates is used as amplification reagent. At the same time, the excellent selectivity of the present biosensor is also confirmed by using three kinds of proteins (BSA, human IgM and human IgE) as controls. These results confirm that MNPs is a powerful sandwich element and an excellent amplification reagent for SPR based sandwich immunoassay and SPR has a great potential for the detection of MNPs-based bioseparation products.

Published by Elsevier B.V.

1. Introduction

Biosensors based on surface plasmon resonance (SPR) spectroscopy have attracted tremendous interest in the past decade, both from a fundamental-physics perspective and as highly sensitive devices for biological studies [1,2], health science research [3–5], drug discovery [6,7], clinical diagnosis [8,9], and environmental and agricultural monitoring [10]. SPR allows the qualitative and quantitative measurements of biomolecular interactions in rapid and real-time environment without requiring a labeling procedure [11]. Furthermore, the kinetic data including the equilibrium constant, the association and dissociation parameters between biomolecules can also be obtained by simulating SPR kinetic curves [12]. Due to these advantages, the biosensor for detecting different kinds of biomolecules including microorganisms [13,14], toxins [15,16], proteins [17,18] and nucleotides [19] had been successfully constructed by SPR spectroscopy. Although these SPR biosensors are selective and can detect large biomolecules, compared with the traditional means, there are still some shortcomings in testing costs, background interference and sensitivity, particularly for the detection of target with very low concentration in real samples.

The emergence of nanotechnology provides an opportunity to increase the sensitivity of SPR for the detection of trace target molecules, among which metal nanoparticle labels with unique optical and electrical properties offer an excellent amplification effect [20]. During the past few years, numerous ultrasensitive SPR biosensors [21–23] had been constructed by combing the amplification effect of Au nanoparticles (Au NPs). Au NPs-conjugated systems have been investigated as a remedy for the detection limit of, or as a feasible enhancement method for SPR signals. Signal enhancements of biomolecule have been achieved successfully by using Au NPs-biomolecules conjugates either as the amplification reagent of sandwich immunoassay or the competitive reagent of indirect competitive inhibition assay [24,25]. The reasons for enhancement are attributed to the higher molecular weight of Au NPs conjugates and the electronic coupling interaction between the Au NPs and the surface plasmon wave associated with the SPR gold film [26,27]. Besides Au NPs, the amplification effect of NPs including SiO_2 NPs [28], Pd NPs [29] and Pt NPs [30] had also been demonstrated for SPR spectroscopy.

More recently, magnetic nanoparticles (MNPs) have been receiving increased attention [31]. As one of the most important nanomaterials in bioanalysis and bioseparation, MNPs have been widely applied in the immobilization and purification of biomolecules due to their larger surface areas which may provide a high density of biomolecule immobilization, and their magnetism which allow targets in clinical samples to be directly captured, easily separated and even concentrated by MNPs [32–37]. However, most of these reports were focused on employing MNPs as special biomolecule immobilizing carriers; the amplification effect of MNPs or using MNPs as labels for enhancing biodetection is sel-

* Corresponding author. Tel.: +1 508 831 5275; fax: +1 508 831 5936.
E-mail address: szhou@wpi.edu (H.S. Zhou).

0039-9140/$ – see front matter. Published by Elsevier B.V.
doi:10.1016/j.talanta.2011.02.020

dom studied, especially in SPR based bioassay. Considering the high refractive index and the high molecular weight of MNPs [38], it is possible to design excellent SPR biosensor by using MNPs as an amplification reagent. Compared with Au NPs, MNPs with controllable size could be easily prepared by the co-precipitation of Fe^{2+}/Fe^{3+} or the hydrothermal decomposition of Fe salts [39–42], which will be economical because of the low cost of Fe salts. Importantly, MNPs can enrich and separate biomolecules from complex sample, which could greatly reduce the background interference of unknown compound in SPR bioassay. Therefore, once the amplification effect of MNPs for SPR spectroscopy is demonstrated, a cost-effective, low-interference and sensitive SPR biosensor will be expected. Furthermore, the characters of MNPs both as the amplification reagent of SPR spectroscopy and the separation carrier of biomolecules could also provide an opportunity to construct the integrated device of MNPs-based-separation and SPR-based-detection.

So far there has been little research reported on the SPR response of MNPs and most of them focus on utilizing commercial strepavidin-conjugated MNPs for signal amplification [43,44]. Although a strong SPR response is observed, biotin is necessary to be attached on SPR substrate surface for the further binding of strepavidin-conjugated MNPs, which limits the extensive application of MNPs in the SPR field. To further understand the SPR response of MNPs and extend the application of SPR in detecting MNPs labeled biomolecules and their separation product, here, we strongly focus on studying the SPR response of the carboxyl group modified Fe_3O_4 MNPs because the carboxyl groups on Fe_3O_4 MNPs allow the MNPs to be easily functionalized by all kinds of biomolecules, which will provide a great potential for the extensive applications of Fe_3O_4 MNPs in SPR based biodetection.

2. Materials and methods

2.1. Materials

2-Mercaptoethyamine, ethanolamine, 6-mercaptohexan-1-ol (MCH), albumin from bovine serum (BSA), FeO(OH), oleic acid, thrombin, N-hydroxysuccinimide (NHS), 1-octadecene, acetone, chloroform, 1-ethyl-3-(3-dimethylaminopropyl)carbodiimide hydrochloride (EDC), poly(maleic anhydride-alt-1-octadecene) (molecular weight: 30,000–50,000) and 2-(2-aminoethoxy)-ethanol were purchased from Sigma and used as received. Sodium hydrogen phosphate heptahydrate, potassium dihydrogen phosphate, sodium borate and sodium chloride were ordered from Alfa Aesar. Human immunoglobulin M (IgM) and human immunoglobulin E (IgE) were ordered from Thermo Scientific (USA). The 5′-thiol or amino-modified aptamers of thrombin were obtained from Integrated DNA Technologies (IDT). The sequences were 5′-SH-C_6-GGT TGG TGT GGT TGG-3′ and 5′-NH_2-C_6-GGT TGG TGT GGT TGG-3′. The aptamer solutions were prepared by dissolving aptamer in 50 mM pH 8.0 Tris–HCl buffer including 138 mM NaCl and 5 mM $MgCl_2$. Protein solutions were prepared by dissolving different proteins in pH 7.4 PBS (10 mM). All glassware used in the experiment was cleaned in a bath of freshly prepared 3:1 HCl:HNO_3 (aqua regia) and rinsed thoroughly in H_2O prior to use (caution: aqua regia solution is dangerous and should be handled with care).

2.2. The synthesis and label of monodispersed, soluble Fe_3O_4 MNPs

Monodispersed Fe_3O_4 MNPs was synthesized by the pyrolysis of iron carboxylate in organic phase [45]. In brief, a mixture of FeO(OH), oleic acid and 1-octadecene was refluxed at 320 °C for 1 h under nitrogen atmosphere. The resulting MNPs were precipitated with acetone and collected by centrifugation at 4000 × *g*. After that, Fe_3O_4 MNPs were further purified by repeated extraction of the precipitate with $CHCl_3$/acetone (1:10) until a powder of Fe_3O_4 MNPs was obtained. Fe_3O_4 MNPs was transferred to PBS solution according to Yu's work with minor modifications [46]. Carboxy group modified amphiphilic polymers was firstly prepared by mixing poly(maleic anhydride-alt-1-octadecene) with 2-(2-aminoethoxy)-ethanol (molar ratio 1:120) in chloroform overnight. Then, the monodispersed Fe_3O_4 MNPs (purified and dispersed in chloroform) was dispersed in the carboxy group modified amphiphilic polymers solution and stirred overnight at room temperature (molar ratio of Fe_3O_4/polymer was 1:10). After that, PBS buffer (pH 8.0, 10 mM) was added to the chloroform solution of the complexes with at least a 1/1 volume ratio; chloroform was then gradually removed by rotary evaporation at 35 °C and water-soluble carboxy group modified Fe_3O_4 MNPs was obtained in clear and dark-purple solution. This transfer process had a 100% efficiency, and no residue was observed. The original concentration of soluble Fe_3O_4 MNPs analyzed by atomic absorption spectroscopy was 301.4 nM, which will be used to prepare other concentration Fe_3O_4 MNPs solution by dilution.

To prepare aptamer–Fe_3O_4 MNPs conjugates, the monodispersed, soluble Fe_3O_4 MNPs were diluted into pH 8.0 PBS buffer with a final concentration of 3 nM, and then, 1 mg EDC and 1 mg NHS dissolved in 5 ml sodium borate (10 mM, pH 5.5) were mixed with 5 ml Fe_3O_4 MNPs solution (3 nM) under stirring for 0.5 h to activate the carboxyl group on the surface of Fe_3O_4 MNPs. After that, 250 μl 35 μM amino-modified anti-thrombin aptamer was added and they are allowed to react for 2 h to immobilize aptamer on the surface of Fe_3O_4 MNPs. After that, 1 M ethanolamine was added for 1 h to block the unreacted carboxyl groups. Then, this solution was centrifuged at 14,000 × *g* at room temperature for 25 min twice to remove the free amino-aptamer. At last, the Fe_3O_4 MNPs was dispersed in 5 ml pH 8.0 PBS buffer and stored at 4 °C.

2.3. In situ SPR measurement

The SPR experiments were done using Eco Chemie Autolab SPR systems [47,48]. It works with a laser diode fixed at a wave-length of 670 nm, using a vibrating mirror to modulate the angle of incidence of the p-polarized light beam on the SPR substrate. The instrument was equipped with a cuvette. Gold sensor disk (25 mm in diameter) was mounted on the hemicylindrical lens (with index-matching oil) to form the base of the cuvette. The cuvette could contain sample with adjustable volume from 10 μl to 1000 μl. An O-ring (3 mm inner diameter) between the cuvette and disk prevents leakage. An auto-sampler (Eco Chemie) with controllable aspirating–dispensing–mixing pipette was used to add samples into the cuvette and provide constant mixture by aspiration and dispensing during measurements. This experimental arrangement maintains a homogenous solution and reproducible hydrodynamic conditions. The inject rate and mixing rate for all samples were 10 μl/s and 40 μl/s, respectively, with the total volume for all samples dispensed in SPR cell equal to 40 μl. This setup allows us to measure the SPR angle shift in millidegrees (m°) as a response unit to quantify the binding amount of macromolecules to the sensor surface.

For detailed experiment, the SPR gold film was initially immersed into the thiol-thrombin aptamer solution for 12 h in order to assemble the monolayer of aptamer by the interaction between Au and thiol group in aptamer. Then the aptamer modified gold film was thoroughly rinsed with 10 mM PBS buffer and water to remove the weakly adsorbed aptamer. Aptamer modified SPR gold film was further immersed in 100 μM 6-mercapto-hexanol for 1 h to block the uncovered gold surface. This gold film was

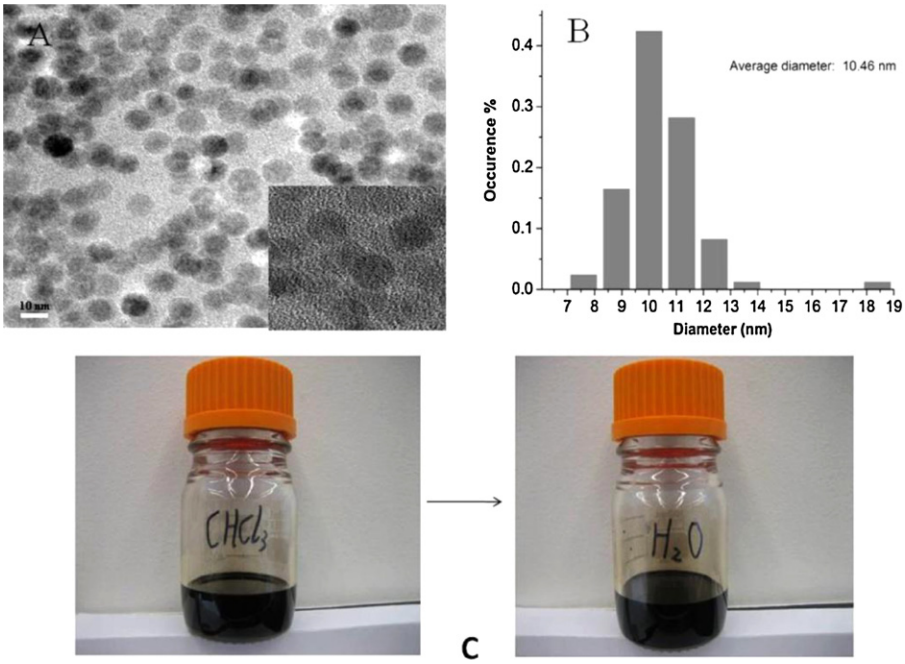

Fig. 1. (A) TEM images of the prepared Fe_3O_4 MNPs and (B) their size distribution. (C) The optical picture of Fe_3O_4 MNPs before and after the phase transference.

used as a sensing surface to detect different concentrations of thrombin by injecting 40 μl thrombin into cell for 10 min. Then the aptamer–Fe_3O_4 MNPs conjugates was added to the SPR cell and react them for 10 min, the unbound aptamer–Fe_3O_4 MNPs conjugates was removed by flow of buffer solution. In order to reduce the disturbance of protein denaturation resulted from the regenerating process for the detecting results, we change a new substrate after each detection. The modification of each of gold substrate is carried out under the same experimental condition.

3. Results and discussion

The essential prerequisite of this study is to synthesize soluble, monodispersed and stable Fe_3O_4. Although soluble Fe_3O_4 MNPs could be easily synthesized by co-precipitation of aqueous Fe^{2+}/Fe^{3+} salt solutions with the addition of a base under inert atmosphere at room temperature or at elevated temperature, the size of the MNPs is not very uniform [39,40]. Furthermore, the prepared Fe_3O_4 MNPs are also easy to aggregate. Fortunately, some references had demonstrated that monodispersed Fe_3O_4 MNPs with controlled size could be synthesized through thermal decomposition of ion compounds in high-boiling organic solvents [41,42]. The prepared Fe_3O_4 MNPs shows a high stability in organic phase due to the protection of oleic acid bound on Fe_3O_4 MNPs surface. Inspired by this kind of synthesis method, here, we synthesize the monodispersed Fe_3O_4 MNPs by the pyrolysis of iron carboxylate in 1-octadecene with oleic acid as protection. Fig. 1A provides the TEM images of the prepared Fe_3O_4 MNPs. It clearly shows the prepared Fe_3O_4 MNPs are spherical. The average size of Fe_3O_4 MNPs derived from their size distribution (shown in Fig. 1B) are ~10.46 nm (n = 300 particles). Importantly, Fe_3O_4 MNPs' size distributions are narrow, which indicates the prepared Fe_3O_4 MNPs is monodispersed. To extend the application of these high-quality Fe_3O_4 MNPs in bioanalysis, it is necessary to transfer these Fe_3O_4 MNPs from organic phase to water phase. Numerous references had demonstrated that amphiphilic polymer is one of the best phase transference reagents because the amphiphilic polymers not only enables the phase transfer of the nanoparticles from organic solvents to aqueous solution, but also serves as a versatile platform for chemical modification and bioconjugation of biomolecules [49,50]. Therefore, poly(maleic anhydride-alt-1-octadecene) after partial acid hydrolysis of 2-(2-aminoethoxy)-ethanol is used as the phase transference reagent to produce soluble carboxyl groups modified Fe_3O_4 MNPs. Fig. 1C shows the optical picture of Fe_3O_4 MNPs before and after the phase transference. The pictures clearly show Fe_3O_4 MNPs possess good stability both in chloroform and water solution. The possible reason comes from the large hydrodynamic size of the polymer coated on Fe_3O_4 MNPs, which inhibit the aggregation of Fe_3O_4 MNPs. These results demonstrate the prepared Fe_3O_4 MNPs possesses a narrow size distribution and a high stability both in organic and water phase, which are all beneficial for the acquisition of accurate and repeated SPR analytical results.

After the high quality Fe_3O_4 MNPs was obtained, the concentration dependent effect of Fe_3O_4 MNPs for SPR was first observed by assembling different concentrations Fe_3O_4 MNPs on 2-mercaptoethyamine (MEA) modified SPR gold film. The thiol group in MEA binds to the Au surface, leaving the amine group free to bind with carboxyl group in soluble Fe_3O_4 MNPs by electrostatic interaction. Fig. 2 illustrates the changes that occur in the SPR angle shift as a function of the concentration for 10.46 nm Fe_3O_4 MNPs. It

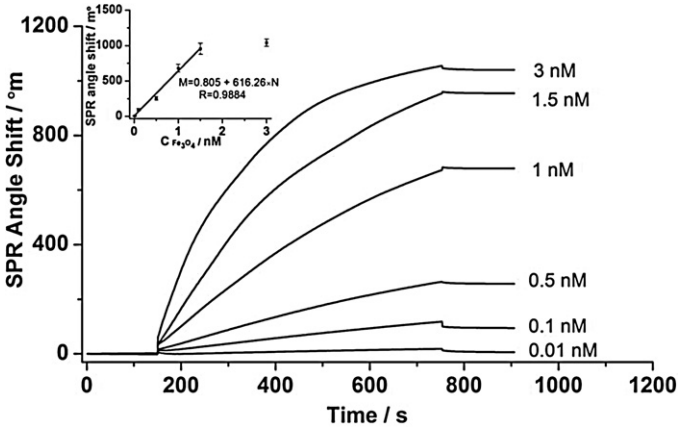

Fig. 2. Variation of SPR angle–time curves with the concentration of Fe_3O_4 MNPs.

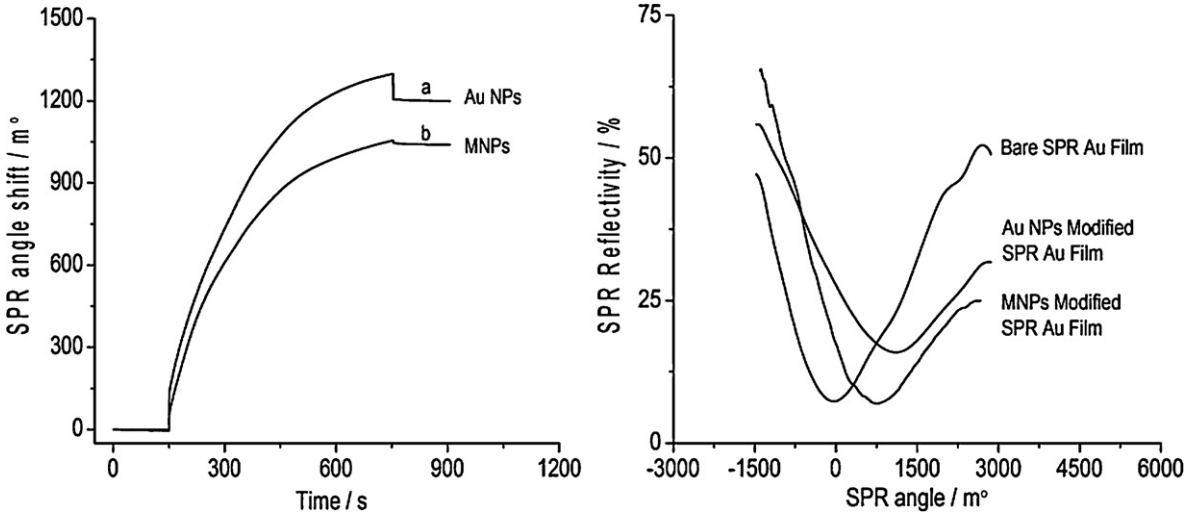

Fig. 3. (A) SPR angle–time curves for in situ observing the adsorption of Au NPs (a) and Fe_3O_4 MNPs (b) on MEA modified SPR gold film. (B) SPR angle–reflectivity curves of bare SPR Au film, Au NPs modified SPR Au film and Fe_3O_4 MNPs modified SPR Au film.

could be easily observed that the SPR angle shifts gradually increase with the increase of Fe_3O_4 MNPs concentration. After analyzing the change of SPR angle shift with the concentrations of Fe_3O_4 MNPs (Shown in the insert in Fig. 2), a linear relation is derived over a range of 0.01–1.5 nM with a correlation factor of 0.9884. The regression equation is $M = 0.805 + 616.24 \times N$ (here, N is the concentration of Fe_3O_4 MNPs and M is the SPR angle shift). Besides that, the saturation adsorption trend could also be observed from the insert in Fig. 2. When the concentration of Fe_3O_4 MNPs is lower than 1.5 nM, the SPR angle shift linearly increased with the increase of Fe_3O_4 MNPs concentration. However, the increase trend of SPR angle shift becomes very small when the concentration of Fe_3O_4 MNPs is increased from 1.5 nM to 3 nM. It indicates a saturation adsorption of Fe_3O_4 MNPs will be approached when the concentration of Fe_3O_4 MNPs is higher than 1.5 nM. Therefore, 3 nM Fe_3O_4 MNPs solution is used in the following experiment to obtain a rapid and sensitive SPR response. It should be pointed out that the SPR angle shift resulted from the adsorption of Fe_3O_4 MNPs is much higher than that of the value resulted from the adsorption of most biomolecules under the same concentration [10,51]. The reason mainly comes from the high refractive index of Fe_3O_4 MNPs [38]. It is well known that materials with higher refractive index could result in a bigger SPR angle shift. Another reason could be attributed to the high molecular weight of Fe_3O_4 both from Fe_3O_4 self and the polymer coated on its surface. Obviously, higher mass change will also result in a bigger SPR response. These results demonstrate the adsorption of Fe_3O_4 MNPs on SPR gold film could result in a great SPR angle shift.

Because the Au NPs has been more accepted as the amplification reagent of SPR spectroscopy, it is necessary to compare the SPR response of Fe_3O_4 MNPs with Au NPs. For this purpose, 3 nM Au NPs with ~13.5 nm diameter and 3 nM Fe_3O_4 MNPs are adsorbed onto MEA modified SPR gold film at the same experimental condition, respectively. Two kinds of monitor modes, SPR angle–time kinetics curve and SPR angle–reflectivity curve, are used to observe the binding of two kinds of NPs onto SPR gold film. The results are shown in Fig. 3. Fig. 3A shows the SPR angle–time kinetics curves, which clearly indicates that the binding of Fe_3O_4 MNPs result in the SPR angle shift of ~1040 m° (curve b in Fig. 3A). This angle shift is a little lower than that of value (~1199 m°) resulted in the adsorption of Au NPs (curve a in Fig. 3A). However, a very interesting phenomenon is found when the SPR angle–reflectivity curve is used to compare the SPR responses of Fe_3O_4 MNPs with Au NPs. As shown in Fig. 3B, the adsorption of Au NPs on SPR gold film results in a big angle shift of SPR resonance angle and an obvious decrease of the depth of the SPR spectrum. The big angle shift of SPR resonance angle can be explained by the strong electronic coupling interaction between the localized surface plasmon of the Au nanoparticles and the surface plasmon wave associated with the SPR gold film. The decrease of the depth of the SPR spectrum could be attributed to the optical loss resulted in the scattering effect of dense Au NPs. These results agree well with the previous report. Compared with the adsorption of Au NPs, the SPR angle–reflectivity curve resulted from the adsorption of Fe_3O_4 MNPs is clearly different. The similar SPR angle shift demonstrates the SPR response of Fe_3O_4 MNPs could be comparable with the SPR response of Au NPs. Importantly, the depth of the SPR spectrum is almost the same before and after Fe_3O_4 MNPs is adsorbed, which indicates the optical loss resulted in the adsorption of Fe_3O_4 MNPs is very small. The possible reason is that the polymer coated on Fe_3O_4 MNPs greatly decrease the conductivity of MNPs because the polymer is highly isolated. Therefore, compared with bare metal NPs, the imaginary part of polymer-coated-MNPs will be very small, which result in a low optical loss. Obviously, the big SPR angle and low optical loss of MNPs are beneficial to increase the high sensitivity of SPR-based biosensor.

To further demonstrate the amplification effect of Fe_3O_4 MNPs and their potential application in SPR sensing, a SPR based ultrasensitive sandwich assay is constructed by using thrombin as the model analyte, which is one of the important component in blood. The principle of SPR biosensor for the detection of thrombin is shown in Fig. 4. Anti-thrombin aptamer is first immobilized on SPR gold film as sensing surface, followed by injection of thrombin into SPR cell for 10 min, and aptamer–Fe_3O_4 MNPs conjugates as amplification reagent to enhance the SPR signal for the detection of thrombin. Different from the general sandwich immunoassay that requires secondary antibody labeled by enzyme or nanoparticles for amplification and detection of protein, here, the application of aptamer–Fe_3O_4 MNPs conjugates as amplification reagent will show more advantages, such as long-term storage and reversible thermodynamic denaturation because both aptamer and Fe_3O_4 MNPs possess high stability. Although the amplification effect resulted by Au NPs–aptamer conjugates is also very good, one inevitable disadvantages coming from Au self is that their testing cost is very high. Compared with Au NPs, Fe_3O_4 MNPs is cost-effective. Furthermore, considering the simplicity of the labeling

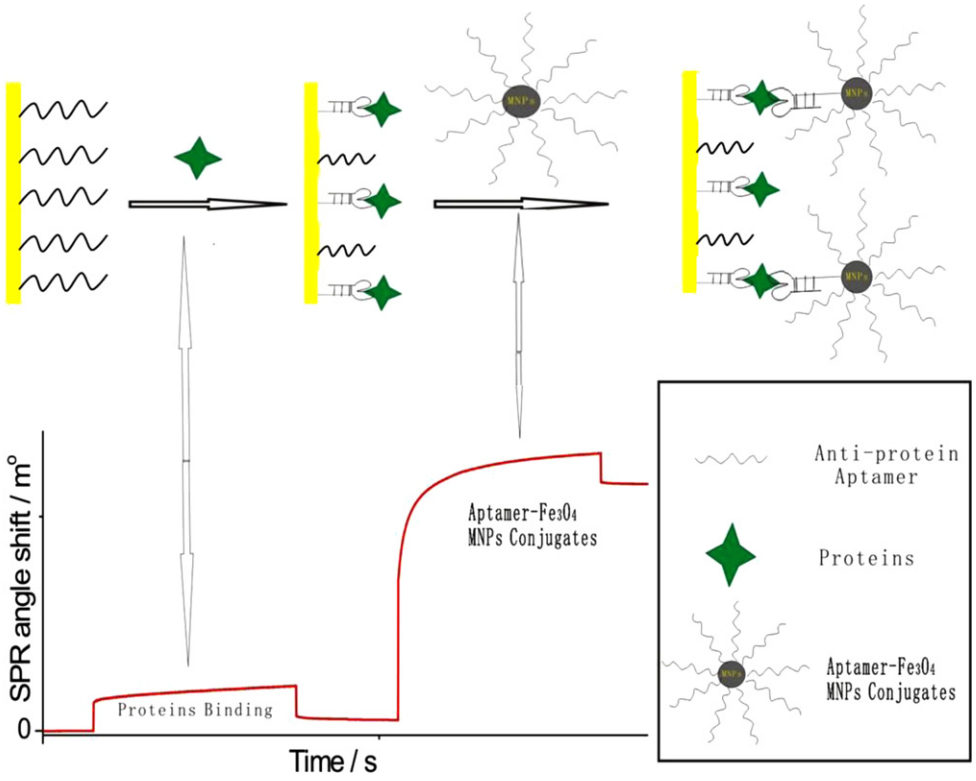

Fig. 4. A schematic representation of the SPR sandwich immunoassay for the detection of thrombin that utilizes aptamer–Fe_3O_4 MNPs conjugates as amplification reagent.

procedure of Fe_3O_4 MNPs over radioisotopic [52], fluorescence [53] and enzyme [54] labels, it is promising that the application of aptamer–Fe_3O_4 MNPs conjugates in SPR field will combine the advantages of immunoassay, aptamer technique, and nanomaterial for increasing the sensitivity of detection, decreasing the testing cost, and extending the type of sandwich immunoassay.

Fig. 5 shows the in situ SPR curves for the detection of thrombin. It could be clearly seen from the phase a in Fig. 5 that the SPR angle shifts gradually increase with the concentration of thrombin concentration increasing from 27 to 2700 nM. However, when

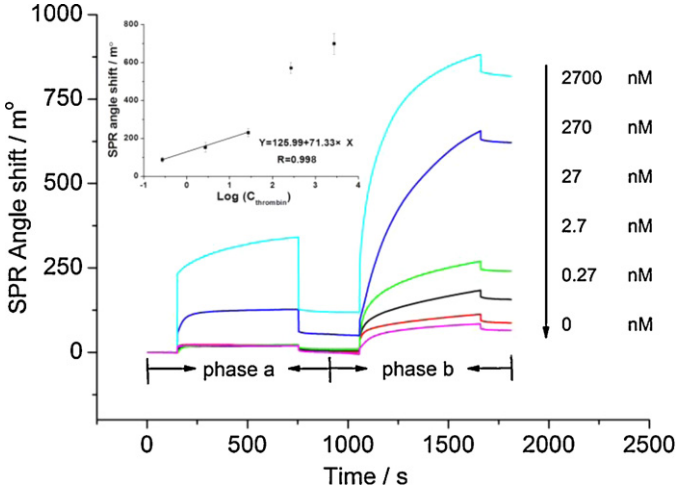

Fig. 5. Representative overlaid sensorgrams illustrating the real-time immunoassay of thrombin at different concentrations (0, 0.27, 2.7, 27, 270, 2700 nM, from bottom to top). Arrows indicate phases of (a) the binding curves of different concentrations thrombin on aptamer modified SPR gold film, (b) after aptamer–Fe_3O_4 MNPs conjugates enhancement. Insert: the relation of SPR angle shift with different concentrations thrombin. The error bars represent average standard errors for three measurements.

the concentration of thrombin concentration is lower than 27 nM, it is very difficult to discriminate the concentration of thrombin concentration by SPR spectroscopy. Obviously, this detection limit is not enough for the detection of thrombin due to the trace amount of thrombin in serum. Thus, we try to amplify the detecting signal of the aforesaid thrombin sensor by using aptamer–Fe_3O_4 MNPs conjugates as an amplification reagent. The availability of this sandwich amplification is based on the fact that there are two binding sites between thrombin and its aptamer. The amplification results of aptamer–Fe_3O_4 MNPs conjugates for SPR signal are shown in phase b in Fig. 5. The figure shows that SPR angle shifts resulted in the binding of aptamer–Fe_3O_4 MNPs conjugates greatly increase with the thrombin concentration, which enables us to detect the trace thrombin. By analyzing the change of SPR angle shift resulted by the adsorption of aptamer–Fe_3O_4 MNPs conjugates with the concentrations of thrombin, a linear relationship between the logarithms of thrombin concentrations and the SPR angle shift over a range of 0.27–27 nM with a correlation factor of 0.998 is deduced (shown in the insert in Fig. 5). The regression equation is $Y = 125.99 + 71.33 \times X$ (here, X is the logarithmic concentration of thrombin (nM) and Y is the SPR angle shift) and the lowest detection limit of this sensor system was 0.017 nM. This detection result is comparable with most other aptasensors [55–58]. Besides sensitivity, the specificity of aptamer promises the selectivity of present SPR sensor for thrombin. Three kinds of proteins (BSA, human IgM and human IgE) are chosen as controls to compare their SPR signal change with that of thrombin. The results are shown in Fig. 6. The red columns in Fig. 6 are the SPR angle shift resulted by the adsorption of different proteins on anti-thrombin aptamer-modified SPR gold film. From these columns, we could easily see the adsorption of BSA, human IgM and human IgE are all very small. By contrast, the adsorption of 100 μg/ml thrombin results in a 118.6 m° of SPR angle shift. The green columns in Fig. 6 are the SPR angle shift resulted by the adsorption of aptamer–Fe_3O_4 MNPs conjugates at different proteins modified SPR gold film. Clearly, the amplification effect of

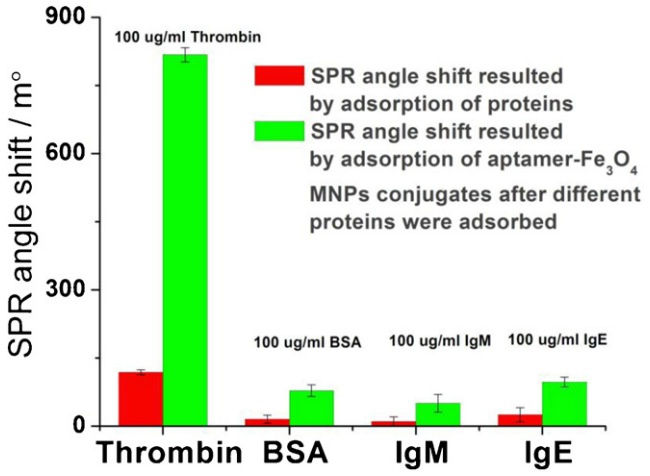

Fig. 6. Specificity analysis of the fabricated SPR biosensor. SPR angle shift resulted by the adsorption of different proteins on anti-thrombin aptamer modified SPR gold film (red columns); SPR angle shift resulted by the adsorption of different proteins on anti-thrombin aptamer modified SPR gold after aptamer–Fe_3O_4 MNPs conjugates enhancement (green columns). The error bars represent average standard errors for three measurements. (For interpretation of the references to color in this figure legend, the reader is referred to the web version of the article.)

aptamer–Fe_3O_4 MNPs conjugates for thrombin is much stronger than for the three control proteins. These results confirm that the present biosensor has a sufficient specificity and thrombin can be identified with high selectivity.

4. Conclusions

In summary, the monodispersed, carboxyl group modified Fe_3O_4 MNPs have been synthesized, and their SPR response onto amino group modified SPR gold substrate has been studied. The results show the monolayer adsorption of Fe_3O_4 MNPs could result in a big SPR signal change with a low optical loss, which provides a new direction to design ultrasensitive sandwich assay by using Fe_3O_4 MNPs as the amplification reagent. To evaluate the practicability of using Fe_3O_4 MNPs in enhancing SPR signal for biosensing, thrombin is used as the model analyte to construct SPR-based sandwich biosensor. The experimental results demonstrate that the addition of anti-thrombin aptamer–Fe_3O_4 MNPs conjugates greatly enhances the sensitivity of SPR sensor for the detection of thrombin with a high selectivity. Importantly, by changing the kind of biomolecules labeled by MNPs, the present detection method will be easy to extend to detect other biomolecules. At the same time, due to the importance of MNPs in bioseparation, the application of MNPs in SPR spectroscopy will provide linkage to fabricating integrated device of rapid separation and in situ detection.

Acknowledgement

The authors greatly acknowledge of the support of this work by the National Science Foundation (EEC-0823974 and CMMI-1030289).

References

[1] R.L. Rich, D.G. Myszka, J. Mol. Recognit. 18 (2005) 431–478.
[2] D.R. Shankaran, K.V. Gobi, N. Miura, Sens. Actuators B: Chem. 121 (2007) 158–177.
[3] B.G.M. Jongerius-Gortemaker, R.L.J. Goverde, F. van Knapen, A.A. Bergwerff, J. Immunol. Methods 266 (2002) 33–44.
[4] I. Mohammed, W.M. Mullett, E.P.C. Lai, J.M. Yeung, Anal. Chim. Acta 444 (2001) 97–102.
[5] E.M. Scherer, M.B. Zwick, L. Teyton, D.R. Burton, Aids 21 (2007) 2131–2139.
[6] U.H. Danielson, Curr. Top. Med. Chem. 9 (2009) 1725–1735.
[7] S.A. Kawamoto, A.D. Thompson, A. Coleska, Z. Nikolovska-Coleska, H. Yi, S.M. Wang, Biochemistry 48 (2009) 9534–9541.
[8] S. Stapleton, B. Bradshaw, R. O'Kennedy, Anal. Chim. Acta 651 (2009) 98–104.
[9] Y. Teramura, H. Iwata, Anal. Biochem. 365 (2007) 201–207.
[10] X.D. Hoa, A.G. Kirk, M. Tabrizian, Biosens. Bioelectron. 23 (2007) 151–160.
[11] J.L. Wang, F. Wang, H.J. Chen, X.H. Liu, S.J. Dong, Talanta 75 (2008) 666–670.
[12] C.T. Campbell, G. Kim, Biomaterials 28 (2007) 2380–2392.
[13] S. Ito, T. Imura, T. Fukuoka, T. Morita, H. Sakai, M. Abe, D. Kitamoto, Colloid Surface B 58 (2007) 165–171.
[14] Z. Zhang, G. Cheng, L.R. Carr, H. Vaisocherova, S.F. Chen, S.Y. Jiang, Biomaterials 29 (2008) 4719–4725.
[15] A.D. Taylor, J. Ladd, S. Etheridge, J. Deeds, S. Hall, S.Y. Jiang, Sens. Actuators B: Chem. 130 (2008) 120–128.
[16] J. Ladd, A.D. Taylor, J. Homola, J. Homola, S.Y. Jiang, Sens. Actuators B: Chem. 130 (2008) 129–134.
[17] A.D. Taylor, J. Ladd, Q.M. Yu, S.F. Chen, J. Homola, S.Y. Jiang, Biosens. Bioelectron. 22 (2006) 752–758.
[18] J. Ladd, H.L. Lu, A.D. Taylor, V. Goodell, M.L. Disis, S.Y. Jiang, Colloid Surface B 70 (2009) 1–6.
[19] C. Boozer, S.F. Chen, S.Y. Jiang, Langmuir 22 (2006) 4694–4698.
[20] L.D. Zhang, M. Fang, Nano Today 5 (2010) 128–142.
[21] L. He, M.D. Musick, S.R. Nicewarner, F.G. Salinas, S.J. Benkovic, M.J. Natan, C.D. Keating, J. Am. Chem. Soc. 122 (2000) 9071–9077.
[22] L.A. Lyon, M.D. Musick, M.J. Natan, Anal. Chem. 70 (1998) 5177–5183.
[23] E. Golub, G. Pelossof, R. Freeman, H. Zhang, I. Willner, Anal. Chem. 81 (2009) 9291–9298.
[24] J.L. Wang, A. Munir, Z.H. Li, H.S. Zhou, Biosens. Bioelectron. 25 (2009) 124–129.
[25] J.L. Wang, A. Munir, H.S. Zhou, Talanta 79 (2009) 72–76.
[26] L.A. Lyon, D.J. Pena, M.J. Natan, J. Phys. Chem. B 103 (1999) 5826–5831.
[27] S. Link, M.A. El-Sayad, J. Phys. Chem. B 103 (1999) 4212–4217.
[28] H.R. Luckarift, S. Balasubramanian, S. Paliwal, G.R. Johnson, A.L. Simonian, Colloid Surface B 58 (2007) 28–33.
[29] K.Q. Lin, Y.H. Lu, J.X. Chen, R.S. Zheng, P. Wang, H. Ming, Opt. Expr. 16 (2008) 18599–18604.
[30] D. Beccati, K.M. Halkes, G.D. Batema, G. Guillena, A.C. de Souza, G. van Koten, J.P. Kamerling, Chembiochem 6 (2005) 1196–1203.
[31] S.X. Wang, G. Li, IEEE Trans. Magn. 44 (2008) 1687–1702.
[32] S. Bi, Y.M. Yan, X.Y. Yang, S.S. Zhang, Chem. Eur. J. 15 (2009) 4704–4709.
[33] C.F. Ding, Q. Zhang, S.S. Zhang, Biosens. Bioelectron. 24 (2009) 2434–2440.
[34] X.L. Chen, Y.F. Huang, W.H. Tan, J. Biomed. Nanotechnol. 4 (2008) 400–409.
[35] H.W. Chen, C.D. Medley, K. Sefah, D. Shangguan, Z.W. Tang, L. Meng, J.E. Smith, W.H. Tan, Chemmedchem 3 (2008) 991–1001.
[36] J.L. Yan, M.C. Estevez, J.E. Smith, K.M. Wang, X.X. He, L. Wang, W.H. Tan, Nano Today 2 (2007) 44–50.
[37] X.L. Zhu, K. Han, G.X. Li, Anal. Chem. 78 (2006) 2447–2449.
[38] D. Grigoriev, D. Gorin, G.B. Sukhorukov, A. Yashchenok, E. Maltseva, H. Moehwald, Langmuir 23 (2007) 12388–12396.
[39] A.H. Lu, E.L. Salabas, F. Schuth, Angew. Chem. Int. Ed. 46 (2007) 1222–1244.
[40] Y.S. Kang, S. Risbud, J.F. Rabolt, P. Stroeve, Chem. Mater. 8 (1996) 2209–2211.
[41] S. Sun, H. Zeng, D.B. Robinson, S. Raoux, P.M. Rice, S.X. Wang, G. Li, J. Am. Chem. Soc. 126 (2004) 273–279.
[42] F.X. Redl, C.T. Black, G.C. Papaefthymiou, R.L. Sandstrom, M. Yin, H. Zeng, C.B. Murray, S.P. O'Brien, J. Am. Chem. Soc. 126 (2004) 14583–14599.
[43] Y. Teramura, Y. Arima, H. Iwata, Anal. Biochem. 357 (2006) 208–215.
[44] S.D. Soelberg, R.C. Stevens, A.P. Limaye, C.E. Furlong, Anal. Chem. 81 (2009) 2357–2363.
[45] W.W. Yu, J.C. Falkner, C.T. Yavuz, V.L. Colvin, Chem. Commun. 20 (2004) 2306–2307.
[46] W.W. Yu, E. Chang, C.M. Sayes, R. Drezek, V.L. Colvin, Nanotechnology 17 (2006) 4483–4487.
[47] J.L. Wang, A. Munir, Z.Z. Zhu, H.S. Zhou, Anal. Chem. 82 (2010) 6782–6789.
[48] J.L. Wang, H.S. Zhou, Anal. Chem. 80 (2008) 7174–7178.
[49] A.P. Zhu, L.H. Yuan, S. Dai, J. Phys. Chem. C 112 (2008) 5432–5438.
[50] B.S. Kim, T.A. Taton, Langmuir 23 (2007) 2198–2202.
[51] W.M. Mullett, E.P.C. Lai, J.M. Yeung, Methods 22 (2000) 77–91.
[52] K. Sundaram, K.G. Connell, Anal. Chem. 47 (1975) 779–780.
[53] C. Orange, A. Specht, D. Puliti, E. Sakr, T. Furuta, B. Winsor, M. Goeldner, Chem. Commun. (2008) 1217–1219.
[54] Y. Zhou, Y. Zhang, C. Lau, J. Lu, Anal. Chem. 78 (2006) 5920–5924.
[55] A.E. Radi, J.L. AceroSanchez, E. Baldrich, C.K. O'Sullivan, Anal. Chem. 77 (2005) 6320–6323.
[56] H. Wei, B.L. Li, J. Li, E.K. Wang, S.J. Dong, Chem. Commun. 36 (2007) 3735–3737.
[57] J. Wang, Y. Cao, G.F. Chen, G.X. Li, ChemBioChem 10 (2009) 2171–2176.
[58] R. Polsky, R. Gill, L. Kaganovsky, I. Willner, Anal. Chem. 78 (2006) 2268–2271.